



Phenomics-enabled prediction of immuno-inflammation drug responses

Immune and inflammatory responses are central to drug efficacy and safety, with dysregulated immune activation underlying adverse events such as cytokine storms, autoimmunity, and chronic inflammation. However, predictive approaches for immune-inflammation liabilities remain limited, often relying on incomplete omics or cheminformatics datasets. In a project supported by the Sanofi iDEA-Tech award, we combined Sanofi's therapeutic interest in immune-inflammation with pixlbio's expertise in highcontent morphological profiling and Al-driven analytics. We developed a domain-specific framework for mechanism-of-action (MoA) and safety prediction of immuno-inflammatory compounds using Phenomics. High-quality, dose-response datasets were generated in multiple immune-inflammation-relevant cell lines, focusing on compounds with well-annotated MoA and safety/toxicity endpoints. Deep learning combined with conformal prediction enabled uncertainty-aware MoA and safety classification, improving predictive accuracy and generalizability. Our fully robotized, iterative workflow demonstrated the feasibility of building high-quality, domain-specific datasets for robust modeling. This collaboration highlights our Phenomics platform as a scalable, Al-driven approach to drug safety and phenotypic screening in immuno-inflammatory drug discovery.



Study design and methods

Study design

- Compound library: 276 compounds were jointly selected. 93 labeled with immuno-inflammation positive mechanism of action (MoA), and 184 immuno-inflammation negative. Doses: 1, 3 and 10µM
- Replicates: 3 technical replicates, 2 biological replicates
- Cell line: A549 lung adenocarcinoma and MRC5 lung fibroblasts
- Plate format: 384 wells

Methods

Cell culture: both cell models were cultured in 384 well plates for high throughput automated processing. pixlbio's automated Cell Painting platform and proprietary optimized protocols and pipelines were used to process a total of 18x384 multiwell plates, generating a total of circa 250.000 images (3Tb), segmenting 5M cells, and extracting 7.5B cellular features at single cell resolution. Image analysis: Cell Profiler was used for Quality Control, as well as image analysis, cell segmentation and feature extraction. Post-processing: Single cell features were aggregated per field of view within a well using the median. Feature selection involved removing highly correlated, low variance and constant features.

Predicting immuno-inflammation: A binary classifier was trained using histogram gradient boosting trees, with each field of view as a sample and compounds annotated with immuno-inflammation MoAs as positives. Predictions were aggregated across concentrations, wells, and fields of view, and across cell lines when applicable. Model evaluation used 20 random stratified compound traintest splits (80%–20%). For each fold, predictions were averaged to produce one score per test compound. Performance was reported as average precision (AP) together with log2 odds lift of AP above baseline

Predicting immuno-inflammation specific MoAs: Separate binary classifiers were trained for each immuno-inflammation MoA using the same setup as the global model. Cross-prediction performance was assessed by comparing how much better each MoA-specific model identified its own MoA versus other MoAs, measured as log2 odds lift in AP. Analysis was limited to nine MoAs with at least three labeled compounds.

Leave-one-out analysis: Global models were retrained while excluding all compounds from one MoA at a time from the train set. This procedure was repeated for the same nine MoAs as above.

Results

Immuno-inflammation compounds induce diverse morphological patterns in both A549 and MRC5 cell lines

For example, the FGFR inhibitor Nintedanib tends to cluster cells, whereas the JAK inhibitor Ruxolitinib produces a subpopulation that shifts from circular to elongated forms in A549 cells.

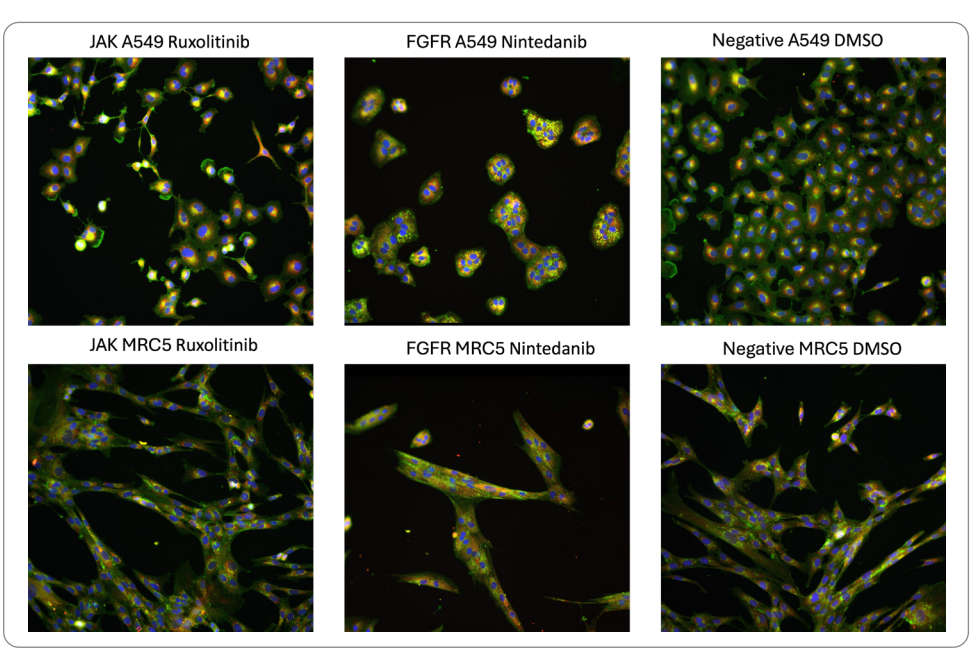


Figure 1: Morphological differences in cells treated with immuno-inflammation compounds. A549 cells (top row) and MRC5 cells (bottom row). Treatments: JAK inhibitor Ruxolitinib (first column), FGFR inhibitor Nintedanib (second column), and DMSO control (last column).



Morphological landscape of A549 and MRC5 cells treated with immuno-inflammation compounds

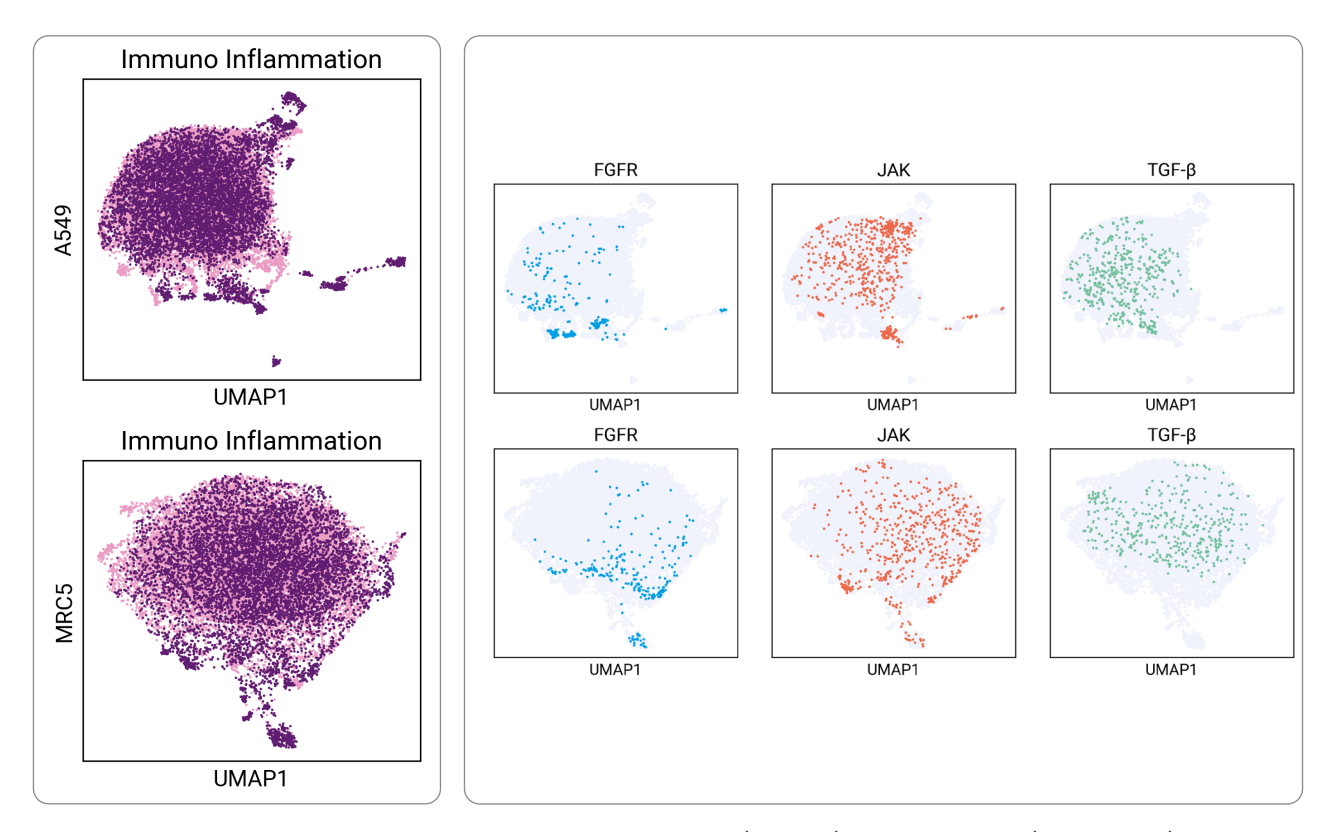


Figure 2: UMAPs of CellProfiler features are shown for A549 cells (top row) and MRC5 cells (bottom row). In the left-most column, all immuno-inflammation compounds (dark purple) are contrasted with negatives (bright pink). The three rightmost columns highlight FGFR, JAK, and TGF-β compounds (colored) against all others (gray).

Immuno-inflammation compounds induce diverse morphological patterns in both A549 and MRC5 cell lines

Immuno-inflammation compounds display consistent effects on cell viability and morphology across both cell lines. MoAs with stronger impacts on viability also tend to produce larger morphological changes. Six MoAs show higher activity, whereas cyclooxygenase, phosphodiesterase, and NFkB inhibitors exhibit weaker effects on both.

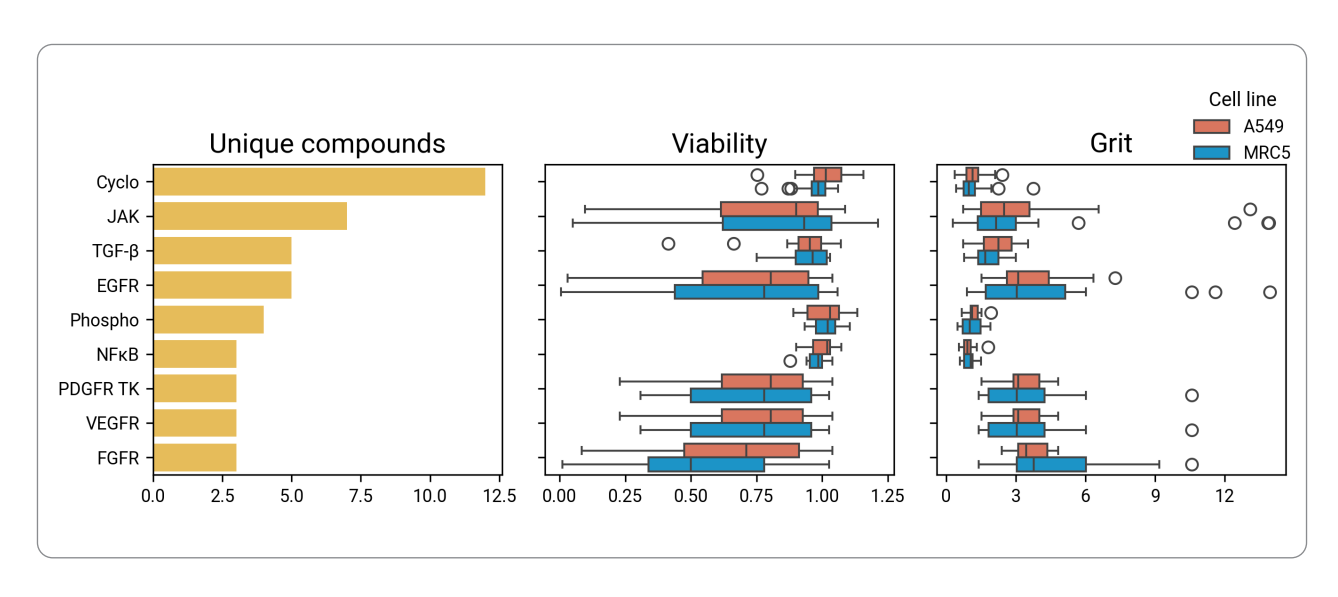


Figure 3: Number of labeled compounds per MoA (left). Distribution of cell viability by compound and MoA (middle). Distribution of grit scores by compound and MoA (right).



Predictive performance of the immuno-inflammation classifier in A549 and MRC5 cells

A model trained on A549 cells achieved an average precision (AP) of 0.54, while models trained on MRC5 cells or on both cell lines reached AP values of ~0.56. This demonstrates that either cell line alone is sufficient for prediction, and that combining them provides a modest gain. The joint model achieved the strongest performance, with a log2 odds lift of 1.36. This corresponds to a 2.5-fold stronger signal relative to baseline, highlighting complementary information across cell lines, even if incremental. Performance further improved when focusing on compounds that induce clearer phenotypic changes. Restricting the test set to compounds with grit scores above 2 yielded a log2 odds lift of ~2.8, underscoring that stronger morphological responses translate into more accurate predictions.

Cell line	AP Baseline	AP Model	Log2 Odds Lift
A549	0.33	0.54	1.25
MRC5	0.33	0.56	1.32
Both	0.33	0.56	1.36

Table 1: Log2 odds lift indicates the improvement in average precision (AP) relative to baseline.

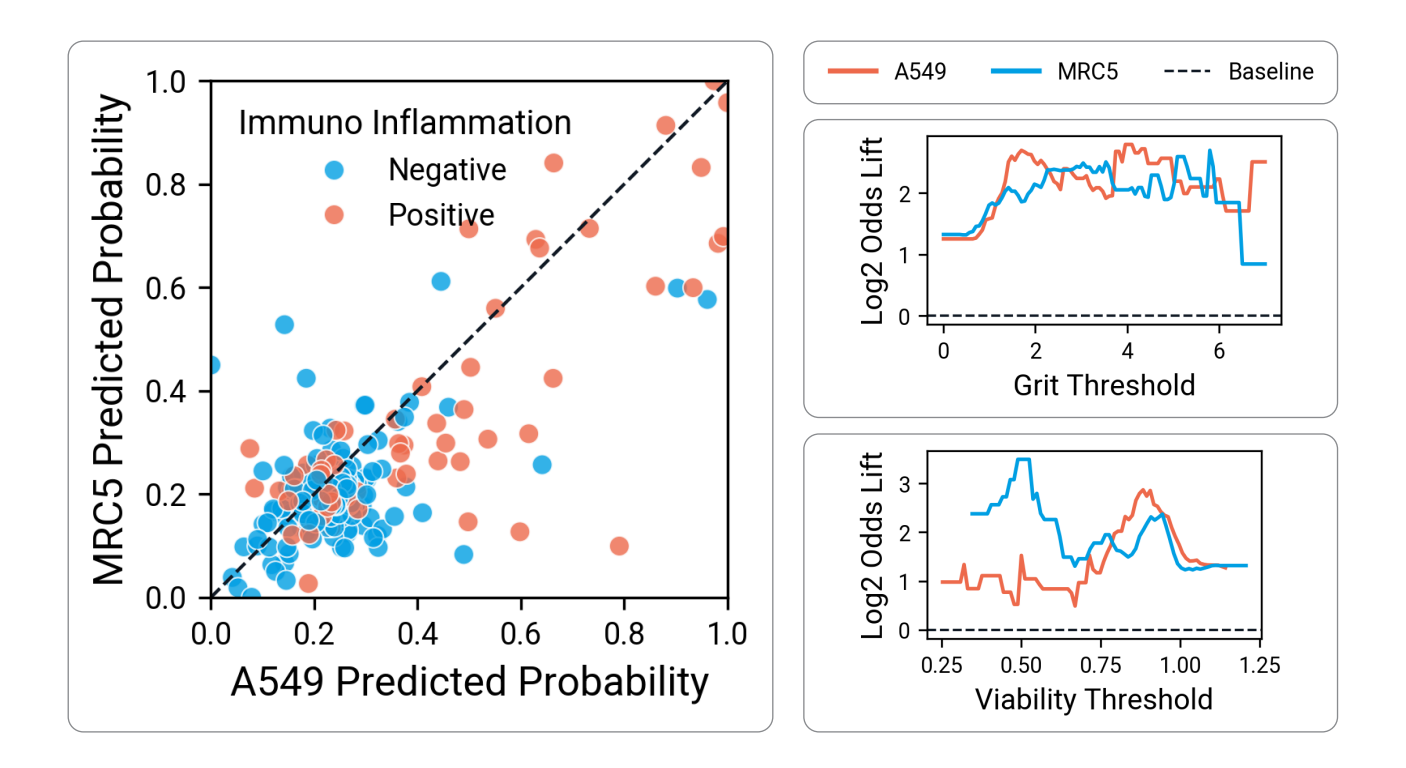


Figure 4: Predictive performance of the immuno-inflammation classifier by cell line, grit score, and viability. A) Predicted probability per compound for a model trained on A549 and MRC5 cells (left). Colored by true positives (red) and negatives (blue). B) Log2 odds lift over baseline when restricting to compounds with higher grit scores (top right) for both cell line models. C) Log2 odds lift over baseline when restricting to compounds with lower toxicity (bottom right) for both cell line models.

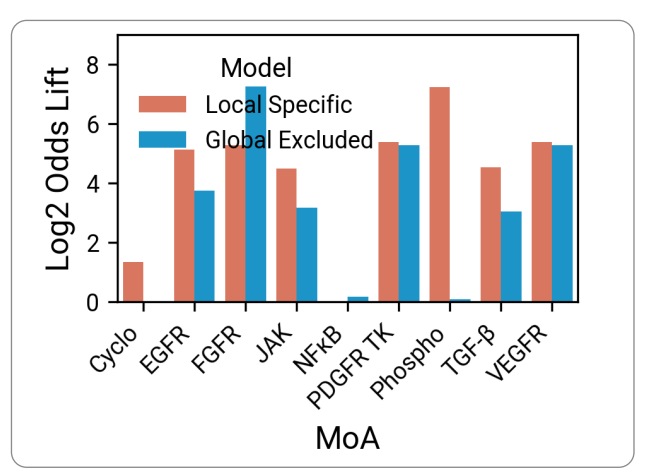


Predictive performance of MoA specific classifiers

Morphological profiles not only predict immuno-inflammation as a whole but also resolve specific MoAs. Phosphodiesterase (PDE) inhibitors are notable: despite low grit scores and minimal effects on viability, PDE was the most accurately predicted MoA. The global model does not generalize to PDE, indicating a distinctive morphological signature that is detectable yet distinct from other immuno-inflammation profiles. Cyclooxygenase (COX) inhibitors show a similar pattern, though with weaker overall performance. Receptor tyrosine kinase classes, EGFR, FGFR, PDGFR, and VEGFR, exhibit broadly similar, high-grit, higher-toxicity profiles, enabling cross-prediction among these MoAs. Even so, they remain separable: for example, the VEGFR-specific model achieves a log2 odds lift of 1.6 when distinguishing VEGFR from FGFR compounds (~3-fold stronger signal).

MoA	AP Baseline	AP Model	Log2 Odds Lift
Cyclo	0.04	0.10	1.33
EGFR	0.02	0.40	5.12
FGFR	0.01	0.32	5.39
JAK	0.03	0.37	4.49
NFĸB	0.01	0.01	0.17
PDGFR TK	0.01	0.32	5.39
Phospho	0.01	0.70	7.24
TGF-β	0.02	0.31	4.54
VEGFR	0.01	0.32	5.39

Table 2: Log2 odds lift indicates the improvement in average precision (AP) relative to baseline.



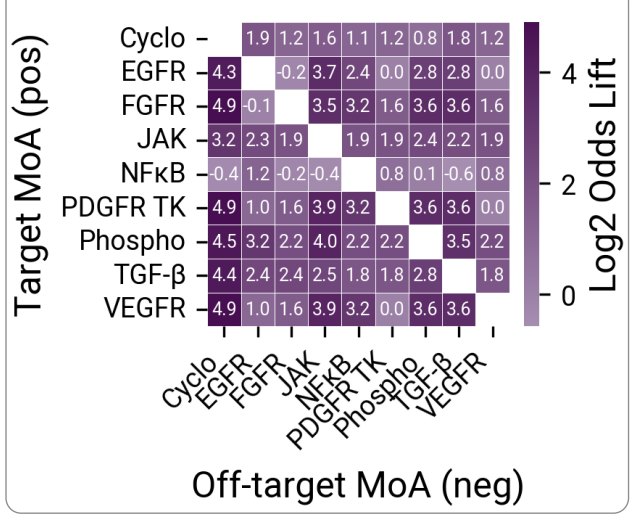


Figure 5: Specificity of MoA specific predictive models. Log2 odds lift relative to baseline for MoA-specific ("local") models versus a global model trained on all immuno-inflammation MoAs except the target. Local models use the target MoA as positives and all others as negatives; the global model excludes the target. The difference indicates how well the target MoA's morphological signature generalizes (left). Cross-MoA specificity of local models. The heatmap shows log2 odds lift when a model trained on a given MoA distinguishes its own class from a single off-target

Conclusions

Our phenomics-based predictive model for immuno-inflammation captures both shared mechanisms and MoA-specific differences. This high-throughput approach markedly reduces the cost and time of immuno-inflammation analysis, enabling faster safety assessments and more efficient compound triaging across all stages of preclinical drug discovery.